Available online at www.sciencedirect.com
SCIENCE DIRECT
ELSEVIER
Polymer 46 (2005) 9974–9986
polymer
www.elsevier.com/locate/polymer

Determination of permeability and diffusivity of oxygen in polymers by polarographic method with inert gas

Jana Wichterlová[a,*], Kamil Wichterle[a], Jiří Michálek[b]

[a]VSB Technical University of Ostrava, 17 listopadu 15, 708 33 Ostrava-Poruba, Czech Republic
[b]Institute of Macromolecular Chemistry, Academy of Science of the Czech Republic, Heyrovského nám. 2, 162 62 Prague 6, Czech Republic

Received 31 August 2004; received in revised form 26 April 2005; accepted 30 June 2005
Available online 19 September 2005

Abstract

A modified polarographic method with inert gas for determination of the oxygen permeability in polymers immersed in liquids is described. Owing to the stream of an inert gas towards polymer from the cathode side, lateral oxygen diffusion (edge effects) is minimized. Unlike the standard Fatt method, the method with inert gas is suitable also for thick samples and, therefore, for high-permeable materials. The method was tested for prediction of oxygen permeability in poly(1-vinyl 2-pyrrolidone) (PVP) and poly(2-hydroxyethyl methacrylate) (PHEMA). As an electrolyte, solution of potassium chloride was used. The effect of additional resistances and small lateral diffusion was taken into account. Unexpectedly, oxygen permeability in both polymers was greater for 0.1 M KCl than for 0.5 M KCl. The experimental setup was also used for diffusivity estimation in thick samples of PHEMA and PVP. Here, the oxygen flux response at one sample surface to the stepwise change in oxygen concentration at the other surface is measured and evaluated. The effect of the additional boundary layer on the oxygen transport is taken into account. A simple procedure for the diffusivity determination from the characteristic time of response as a function of the sample thickness is given. Solubility of oxygen in polymer is calculated from the obtained permeability and diffusivity.

Keywords: Oxygen permeability; Oxygen diffusivity; Polarographic method

1. Introduction

Oxygen transfer in polymers is important in such areas as biocompatible polymers, packaging materials and some membrane processes. A better understanding of the transfer mechanism can contribute to a better strategy of polymer design.

Material properties which determine the oxygen flow through polymer are oxygen diffusivity D and permeability $P=Dk$. Oxygen solubility k cannot be determined directly, thus the characteristics are obtained from suitable diffusion experiments, permeability from the steady state, diffusivity from the unsteady state data. Oxygen flux is mainly measured by a polarographic method.

Oxygen permeability of biocompatible polymers is mostly determined by the standard Fatt polarographic method [1], but the non-idealities (boundary resistances and edge effects) are the reasons why polymer samples should not be thicker than 0.4 mm for a cathode diameter of 4 mm and not more permeable than 75×10^{-11} (cm^2/s)(cm^3 O_2/(cm^3 hPa)), i.e. 100 barrer units.

Even for these thin samples, it is necessary to correct permeability for both types of the non-idealities.

Appropriate formulas [1] for thin samples or cathode divided by narrow insulation (permeometer with guard ring cell, Rehder Development Co., [2]) can be used for elimination of edge effects. Nevertheless, the width of the offered outer guard ring is about 0.7 mm, therefore it is also suitable only for thin samples. The choice of a wider ring would bring another problem because an increasing amount of ions at the cathode would have to migrate to an ambient electrolyte.

Several resistances in series to oxygen flux are usually present. The main additional boundary resistances arise in liquid boundary layers and in a thin wet paper, which has to be inserted between non-hydrogel polymer and cathode. To obtain satisfactory results, the polymer resistance should be dominant. As the polymer resistance is proportional to the

* Corresponding author. Tel.: +420 596 994 328; fax: +420 596 918 647.
E-mail address: jana.wichterlova@vsb.cz (J. Wichterlová).

0032-3861/$ - see front matter © 2005 Elsevier Ltd. All rights reserved.
doi:10.1016/j.polymer.2005.06.125

material thickness and inversely proportional to permeability, it is difficult to satisfy the above condition for thin samples of high-permeable polymers. There are several ways to separate the effect of boundary resistance. The standard ISO procedure [1] recommends multiple measurements of oxygen permeability of the same material at different thickness. But such samples are usually unavailable at the stage of new material development. The repeated measurements with a single sample and different number of wet papers [3] or with a single sample and varying thickness of the top water layer [4] cannot give adequate results for a thin sample of a high-permeable polymer; in that case the above condition is not fulfilled.

In literature, in contrast to many experimental data for permeability, diffusivity is measured infrequently and mostly for thin membranes [5–8]. The effect of a possible additional boundary layer on oxygen transport is not usually considered, which may be source of errors, particularly for high-permeable polymers and thin samples.

In the proposed polarographic method, the inert gas suppresses the lateral diffusion in the polymer sample, the edge effects are smaller and well-defined and one-directional diffusion can be assumed also in thicker samples. In thicker samples, a chance to obtain the dominant resistance in the polymer increases even for high-permeable polymers.

2. Theoretical

2.1. Permeability determination—steady state diffusion

Steady-state one directional diffusion of oxygen through a flat polymer sample of area A and thickness h is expressed as

$$J_s = P\frac{p - p_c}{h}A \tag{1}$$

where J_s is the oxygen molar flow rate, $(p - p_c)$ is the partial pressure difference of oxygen over the sample and the proportionality coefficient, P, is the oxygen permeability in the polymer. By comparison of Eq. (1) with Fick and Henry laws, the P is given by

$$P = Dk \tag{2}$$

where D is the oxygen diffusivity and k is the oxygen solubility in the polymer. Determination of permeability requires the oxygen flow, J_s, to be measured at known $(p - p_c)$.

Unlike for the other gases, the polarographic method popularized by Fatt [9] is suitable for oxygen. The cathode is placed on one surface of the sample. Here, under limiting diffusion current conditions, any oxygen is reduced by the reaction

$$O_2 + 2H_2O + 4e = 4OH^-$$

which means that the partial pressure of oxygen at the cathode is equal to zero,

$$p_c = 0 \tag{3}$$

and, according to Faraday's law, the steady-state electric current, i_s, is

$$i_s = J_s zF \tag{4}$$

where for the above four-electron reaction $zF = 4 \times$ 96,485 C/mol.

Then the following relation follows from Eqs. (1)–(4)

$$\frac{i_s}{zF} = \frac{Ap}{h/P} \tag{5}$$

where now A is the cathode area. Therefore in an ideal case, permeability P can be determined from measured i_s and h.

However, three kinds of non-idealities cannot be usually neglected:

(i) There is some additional resistance in the electrolyte layer on both sides of the sample to oxygen flow; therefore, the partial pressure p is not associated with the sample layer itself.
(ii) The oxygen flow differs from the theory (1) due to the situation at the cathode perimeter, where lateral diffusion may also be significant as Fig. 1(a) shows.
(iii) There is even some current in the oxygen-free environment, i.e. the background current i_b, which contributes to the measured value. It can be caused by the reduction of undesirable electroactive substances.

The current i_b was determined by polarographic experiment with nitrogen and its value was subtracted from all subsequent current measurements.

Obviously, an increase in sample thickness suppresses the effect of additional resistance but it simultaneously causes an increase in lateral diffusion.

For thin samples $h/d < 0.1$, where d is the cathode diameter, the following procedure is offered in the standard method by Fatt [1]. The modified equation

$$\frac{i_s}{zF} = \frac{(1 + \varphi)Ap}{\frac{h}{P} + R_a} \tag{6}$$

includes the above non-idealities.

Dimensionless parameter φ expresses the effect of lateral diffusion; it depends on geometrical configuration of the system and a simple estimate

$$\varphi = 1.89\frac{h}{d} \tag{7}$$

has been recommended in Ref. [1].

Parameter R_a describes the overall additional boundary resistances, which are added to the sample resistance h/P. For thin samples, it is not possible to assume, that the sample resistance is dominant. But under careful control of

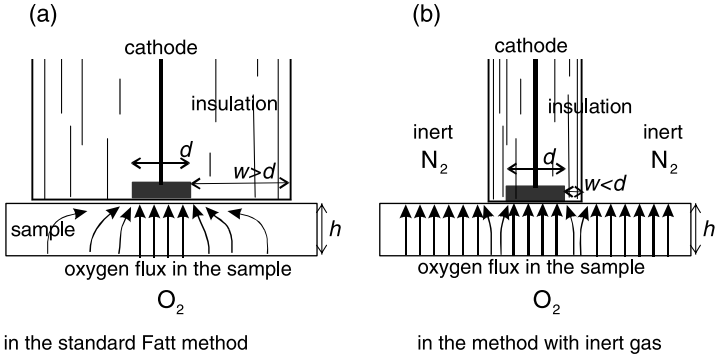

Fig. 1. Oxygen diffusion (a) in the standard Fatt method (b) in the method with inert gas.

experimental conditions (paper thickness, hydrodynamic conditions at the sample surface, etc.), the resistance R_a can be assumed to be constant at least for a certain set of experimental runs with samples of the same polymer with different h.

Then permeability P is evaluated from the dependence of $1/i_s$ on h, Eq. (6), for each such set of runs, but the procedure becomes very laborious.

On the other hand, in the proposed method with inert gas, the edge effects are suppressed (Fig. 1(b)), the sample resistance can be made dominant in much wider conditions and, therefore, R_a can be estimated from Eq. (6) only by one calibration.

2.2. Diffusivity determination—unsteady state diffusion

The diffusivity can be evaluated from the measured time dependence of oxygen molar flow rate $J(t)$ from one surface of a flat polymer sample after a stepwise change of ambient oxygen concentration at the other sample surface [5–8,10–11].

When the step change in oxygen partial pressure from p_0 to p_1 is performed, the oxygen flow rate changes from the initial steady-state value J_{s0} to the final steady-state value J_{s1} (Fig. 2). Then the normalized dimensionless response $\eta(t)$

$$\eta(t) \equiv \frac{J(t) - J_{s0}}{J_{s1} - J_{s0}} \tag{8}$$

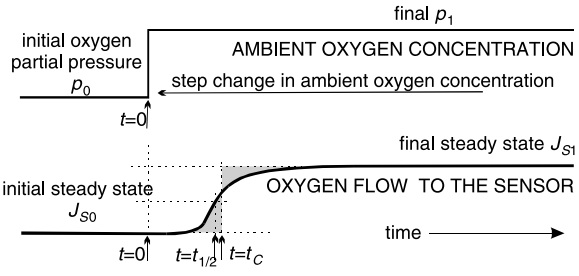

Fig. 2. Dynamic experiment for diffusivity estimation; characteristic time t_C and half-time $t_{1/2}$ of the oxygen flow rate response.

increases from 0 to 1 not depending on particular values p_0 and p_1.

Some typical times of oxygen transfer through the sample can be obtained from the response. For example, the characteristic time t_C in accordance with Aiba [6],

$$t_C \equiv \int_0^\infty [1 - \eta(t)]\mathrm{d}t \tag{9}$$

or the half-time $t_{1/2}$

$$\eta(t_{1/2}) \equiv \frac{1}{2} \tag{10}$$

can be defined. In the time $t = t_C$, two hatched areas in Fig. 2 are equal. The half-time $t_{1/2}$ is the time required for half of oxygen flow rate to be reached; it can be easily estimated from the response.

2.2.1. One-layer model

Theoretical solution [7,8,10] of the simplest case of one-directional unsteady diffusion through the flat sample of constant diffusivity D and thickness h gives the following expressions for the normalized response

$$\eta(t) = 1 + 2\sum_{n=1}^{\infty} (-1)^n \exp\left(-(\pi n)^2 \frac{t}{6t_C}\right) \tag{11}$$

where

$$6t_C = \frac{h^2}{D} \tag{12}$$

and

$$t_{1/2} = 0.8328 t_C \tag{13}$$

The characteristic time t_C can be easily obtained from the experimental response using Eqs. (9) or (13), or by fitting the experimental response $\eta(t)$ with the theoretical one, Eq. (11).

Then the unknown parameter, diffusivity D, can be calculated from Eq. (12) for known t_C.

2.2.2. Two-layer model

Actually, concentration step occurs in an ambient gas or liquid bulk. Mass transfer through a stagnant layer at the sample surface may retard the oxygen flux response. Other retardation may be due to the diffusion through a layer between the sample and oxygen sensor. Therefore, the characteristic time is larger than the one for one-layer case, $6t_C \geq h^2/D$, Eq. (12).

The simple two-layer model schematically shown in Fig. 3, considers all additional effects concentrated in a single additional layer. Parameters related to the additional layer, thickness h_a, oxygen diffusivity D_a, oxygen permeability $P_a = D_a k_a$ and/or oxygen solubility k_a, should be taken into account. They are generally dependent on experimental conditions.

Unsteady one-directional diffusion through the two layers can be described by a set of two partial differential equations. The model was first analyzed by Aiba and Huang [5] using the generalized method suggested by Carslaw an Jaeger [10]. A review of various approaches to the problem is presented by Linek et al. in Ref. [12].

The solution can be described by diffusion resistances

$$R \equiv \frac{h}{P}, \quad R_a \equiv \frac{h_a}{P_a} \tag{14}$$

and diffusion capacities

$$C \equiv \frac{hP}{D}, \quad C_a \equiv \frac{h_a P_a}{D_a} \tag{15}$$

in the form

$$\eta(t) = 1 + 2\sum_{n=1}^{\infty} (-1)^n B_n \exp\left(-(\pi n \beta_n)^2 \frac{t}{6t_C}\right) \tag{16}$$

where now the characteristic time is

$$6t_C = RC + R_a C_a + 2\frac{C + C_a}{\frac{1}{R} + \frac{1}{R_a}} \tag{17}$$

It is seen that the importance of the terms in Eq. (16) decreases with increasing n and Eq. (16) is formally equivalent to Eq. (11) for $\beta_n = 1$, $B_n = 1$, $n = 1, \ldots, \infty$. Eigenvalues β_n and coefficients B_n depend on relative resistance, R_a/R, and on relative capacity, C_a/C. The procedure for calculation of a set of β_n and B_n is described in detail by Linek et al. [11].

The calculated values of β_n and B_n, $n = 1, 2, 3$ for a wide range of R_a/R and C_a/C are given in Table 1. Table 1 shows that for the range $(R_a/R) < 0.1$, which can be expected in diffusion experiments with thick samples, the most important B_n and β_n are close to unity. Thus, the difference of the values $\eta(t/t_C)$ obtained by (11) and (16) is mostly less than 1%. The ratio $t_{1/2}/t_C$ is also presented and it is evident that Eq. (13) is adequate for a wide range of parameters.

Therefore, the simple relation (11) instead of (16) can be accepted. Then the responses $\eta(t/t_C)$ are similar and the value of t_C is obtained from the experimental response as for the one-layer case, e.g. according to Eq. (13).

The oxygen permeability P and possibly the additional resistance R_a is determined from the steady-state data (Section 2.1).

The characteristic time t_C can be used for estimation of the remaining unknown parameters D and D_a from Eq. (17) in the following way. The diffusivity D_a is eliminated by multiple measurements of responses for the same polymer at different thickness h. For this purpose, Eq. (17) with respect to Eqs. (14) and (15) is written in the form

$$6t_C = \frac{1}{D}(h + R_a P)^2 + 3\left(R_a C_a - R_a^2 \frac{P^2}{D}\right)\left(1 - \frac{2}{3}\frac{1}{1 + (h/P)/R_a}\right) \tag{18}$$

It is seen that the value of the expression in the last parentheses of Eq. (18) lies in the interval from 1/3 to 1. Moreover, if the $R_a/R = R_a/(h/P) < 1$, then the actual value of h plays a small role in the last term and the resulting relation for the diffusivity D estimation is

$$6t_C = \frac{1}{D}(h + R_a P)^2 + 3\left(R_a C_a - R_a^2 \frac{P^2}{D}\right) \tag{19}$$

$$\text{for } \frac{R_a}{h/P} < 1$$

Eq. (19) describes the linear dependence of $(6t_C)$ on the square of the effective thickness $(h + R_a P)$; the slope of the line is equal to the reciprocal value of the unknown parameter D and the intercept is a function of the group of unknown variables $R_a C_a = h_a^2/D_a$.

For thicker samples, the condition $R_a/R < 1$ is mostly met but the lateral diffusion becomes more important and the assumption of one-directional diffusion may not be satisfied.

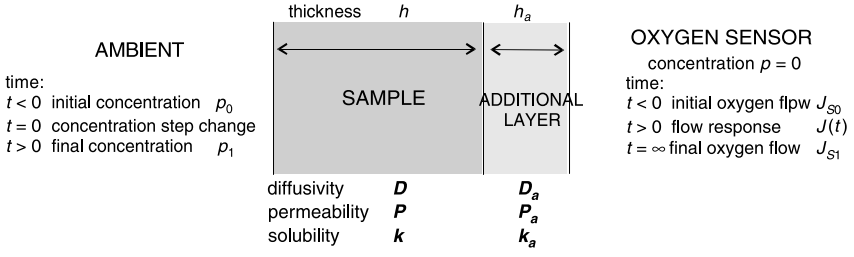

Fig. 3. Two-layer model.

Table 1
Eigenvalues β_n, coefficients B_n of Eq. (16) and $t_{1/2}/t_C$ in dependence on R_a/R, and C_a/C

R_a/R	S[a]	C_a/C	β_1	β_2	β_3	B_1	B_2	B_3	$t_{1/2}/t_C$
0	[b]	0	1.0000	1.0000	1.0000	1.0000	1.0000	1.0000	0.8327
0.05	0.5	0.2	1.0087	1.0052	0.9984	1.0308	1.1275	1.2988	0.8359
0.1	0.5	0.4	1.0262	0.9969	0.9482	1.1019	1.3893	1.5714	0.8436
0.2	0.5	0.8	1.0498	0.9225	0.9235	1.2264	1.3255	1.0667	0.8533
0.3	0.5	1.2	1.0408	0.9114	0.9862	1.1864	1.1400	1.0445	0.8496
[b]	1	[b]	1.0000	1.0000	1.0000	1.0000	1.0000	1.0000	0.8327
0.05	2	0.0125	0.9978	0.9985	0.9997	0.9925	0.9711	0.9386	0.8319
0.1	2	0.025	0.9930	0.9977	1.0039	0.9759	0.9138	0.8347	0.8290
0.2	2	0.05	0.9819	1.0035	1.0250	0.9375	0.8059	0.6878	0.8244
0.3	2	0.075	0.9725	1.0165	1.0516	0.9056	0.7369	0.6311	0.8203
0.05	20	0.000125	0.9971	0.9981	0.9996	0.9900	0.9618	0.9195	0.8319
0.1	20	0.00025	0.9907	0.9967	1.0045	0.9681	0.8869	0.7854	0.8290
0.2	20	0.0005	0.9754	1.0024	1.0281	0.9171	0.7436	0.5846	0.8227
0.3	20	0.00075	0.9615	1.0152	1.0568	0.8730	0.6406	0.4693	0.8149

[a] Parameter $S \equiv (D_a/D)^{1/2}/(P_a/P) = [(R_a/R)/(C_a/C)]^{1/2}$ is independent of material thickness.
[b] Valid for any value.

Therefore the polarographic method with inert gas, which suppresses the lateral diffusion, is suitable.

3. Experimental—the polarographic method with inert gas

3.1. Apparatus and samples

In our experimental set-up, Fig. 4, the polymer sample is fixed water-tightly in a polypropylene diffusion cell. The diffusion cell, oxygen infusion system, temperature sensor and magnetic stirrer are placed in a 250-ml glass beaker. The beaker rests on a magnetic stirrer drive unit. Both the beaker and the diffusion cell are filled with electrolyte. Temperature in the beaker is maintained at 34.5 ± 0.5 °C by the controller.

Electrodes and nitrogen infusion system are placed in the diffusion cell. Nitrogen maintains practically zero oxygen concentration at the upper sample surface even when cathode is absent.

The 24-carat circular gold cathode is sealed in a poly(methyl methacrylate) rod. Therefore, the narrow insulating ring is around the polished gold face. The cathode size and width of the ring were measured with a microscope. A silver wire spiral is the Ag/AgCl anode. The predetermined potential difference, 0.7 V, is set on electrodes.

Transducer converts the measured microampere-level current to the normalized voltage signal. The signal is recorded and the potential difference between the electrodes is controlled by PC software LabView.

The same electrolyte is in the beaker and in the cell. At first, an 0.5 M solution of potassium chloride was used, like in the experiments made by Fatt, Aiba, Nicodemo [1,5,6]. Later on, at greater current intensities, the silver coating appeared on the cathode. Therefore, 0.1 M KCl was chosen, as used by Compan, Weissman [4,13].

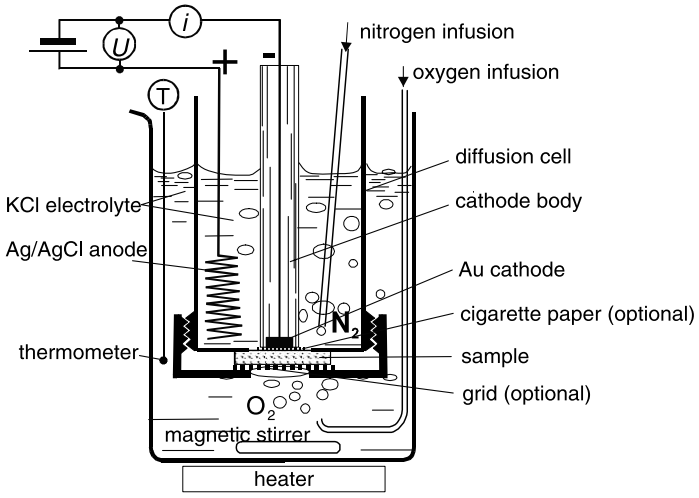

Fig. 4. Experimental set-up for the method with inert gas.

The inlet gases are saturated with water at 35 °C and their flow rates are measured. The bottom shape of the diffusion cell and suitable stirring cause that a large pulsating gas bubble is formed at the lower sample surface and oxygen passes through it to the sample.

Oxygen pressure p was calculated from the measured atmospheric pressure p_{atm} and known partial pressure of water vapor at 34.5 °C, $p_w = 54.7$ hPa, according to the following equation

$$p = p_{atm} - 54.7 \text{ [hPa]} \quad (20)$$

A set of planar samples with different thickness was made by lathe cutting from PVP and PHEMA. After swelling, the samples contained 68 and 38% water, respectively, as checked by refractive index measurement.

To prevent deformation and damage of thin samples, a sparse grid may optionally support the soft ones. Insertion of a piece of wet cigarette paper keeping a defined electrolyte layer on the sample is inevitable for non-hydrogel polymers only. Nevertheless, its effect on the whole boundary resistance was tested with the above samples, too.

The experimental conditions are summarized in Table 2.

3.2. Potential difference and background current

Polarograms were obtained in our experimental set-up with different oxygen concentration in the beaker and always with nitrogen in the diffusion cell. The measured steady-state currents versus applied potential differences for nitrogen, air and oxygen are plotted in Fig. 5 for a PVP sample, $h = 0.950$ mm. It is seen that the value 0.7 V is a reliable potential difference to apply between both electrodes in order to obtain a limiting diffusion regime.

In the presence of nitrogen on both sides of the sample, the value of background current

$$i_b = 0.08 \text{ μA} \quad (21)$$

was found at 0.7 V.

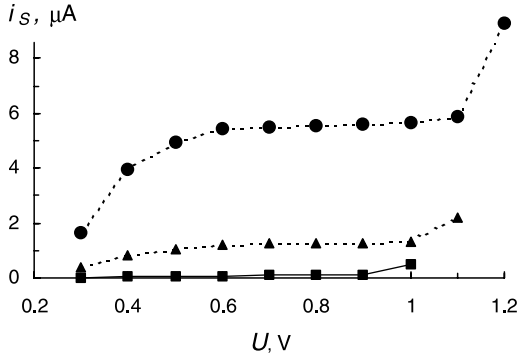

Fig. 5. Polarograms in nitrogen-saturated electrolyte inside the diffusion cell and the following gases in the beaker (●) oxygen, (▲) air, (■) nitrogen.

3.3. Permeability

3.3.1. Procedure

First, the sample was immersed for at least 2 h into an electrolyte. Then anode and the sample, optionally equipped by a sparse grid and in some experiments covered by wet cigarette paper, were carefully fixed in the diffusion cell. The beaker and cell were filled with electrolyte. The cell together with the sample and anode was immersed in the beaker. Nitrogen was introduced into the diffusion cell and oxygen into the beaker.

The start-up period with stirring in controlled temperature environment took about 60 min to approach a steady-state oxygen flow. Then the cathode was immersed ca. 1 cm above the sample in the cell, the potential difference 0.7 V was set on electrodes, the cathode was adjusted to the sample and the diffusion current was recorded. The steady state current can be usually read after another 20 min.

To have a constant boundary resistance, all settings (cell and gas input positions, stirring speed, gas flow rates, etc.) were kept constant for all experiments.

3.3.2. Correction on the edge effects

Construction of our cathode body with insulating ring around the gold cause, that small edge effects have to be

Table 2
Common experimental conditions

Cathode material	Gold, 24 carat
Cathode diameter, d	2.97 mm
Width of insulating ring, w	1.0 mm
Anode material	Pure silver/electrolytic AgCl
Anode area	350 mm^2
Optional extra resistance	Thin sparse grid, wet cigarette paper
Potential difference	0.7 V
Background current, i_b	0.08 μA
Electrolyte	0.5 M KCl, 0.1 M KCl
Temperature in the electrochemical cell	34 ± 0.5 °C
Samples	Hydrogels: PHEMA (38% water), PVP (68% water)
Thickness of the sample, h	0.1–3.1 mm
Sample diameter	15 mm
Atmospheric pressure, p_{atm}	980–1005 hPa

considered also in our method with inert gas. From the theoretical point of view, the edge effects can be avoided by minimization of the ring width w (Fig. 1(b)). However, our experience with a considerably reduced width revealed pulsation of the current. The pulsation was probably caused by non-ideal adherence of cathode to the sample and electrolyte convection induced by nitrogen bubble formation. Therefore, the ring width $w=1$ mm is used, where, of course, the correction φ is not negligible.

A set of φ values was calculated by numerical solution of partial differential equation of the steady-state diffusion with appropriate boundary conditions using a CFD solver Fluent for the parameters under interest. It can be assumed, that for the cathode with insulation, φ is a function of two geometric simplexes, w/d and w/h, where h is the sample thickness and d is the cathode diameter. We have succeeded with the data fitting by a simple interpolation formula [14]

$$\varphi \approx 1.75\frac{w}{d}\left(1-\exp\left(-1.25\frac{h}{w}\right)\right) \tag{22}$$

Fig. 6 shows good agreement between the theoretical and interpolated values.

3.3.3. Fast measurement without the edge effects

During the start-up period, steady-state oxygen transfer in the sample was established only with oxygen and nitrogen, i.e. without support of electrochemical process.

For that reason it can be expected that at the moment when the cathode is attached to the sample, the instant current, i_{min}, corresponds just to the diffusion without edge effects. Later of course, the current has to increase to a new steady-state value i_s due to the developing small lateral diffusion. Therefore, when the value i_{min} is determined, no correction for the edge effect is required ($\varphi=0$) and the electrochemical measurement can be completed in few seconds.

But actually, the used procedure, i.e. to immerse the cathode into the electrolyte near to the sample, to set voltage on it and then to fix it at the sample, did not work well. The typical time dependence of the current is seen in Fig. 7. Electrolyte in the cell is stirred with nitrogen. The cathode in the stirred deoxygenated electrolyte exhibits high current (as high as 2.5 μA in our experiments), which increases with stirring intensity. The convective motion in the electrolyte is particularly significant in the last moment of approaching the cathode to the sample, and current peak appears here. Then the current quickly decreases to the minimal value. But the minimal current data are too scattered (Fig. 8) as the measured i_{min} is a result of several fast competitive processes. Apparently, this promising procedure needs further improvement to provide more reliable data.

3.4. Diffusivity

The diffusivity measurement starts from the initial steady state by switch of the gases, either air–oxygen or oxygen–air. The current response from i_{s0} to i_{s1} is recorded until the final steady state is reached.

Because an electric current i is proportional to the oxygen flow J according to Faradays law (4), the normalized response $\eta(t)$ has a form

$$\eta(t)=\frac{i(t)-i_{s0}}{i_{s1}-i_{s0}} \tag{23}$$

the characteristic time t_C is determined from $\eta(t)$ and the diffusivity D can be estimated according to the procedure described above.

To obtain an appropriate value of diffusivity, almost ideal step in oxygen concentration is essential. This can be more precisely achieved in gas alone, but then maintaining a constant temperature in the sample is less efficient. Both the requirements are accomplished in our apparatus; the detail of the experimental set-up is schematically shown in Fig. 9.

The temperature of the ambient liquid is controlled. A large gas bubble surrounded by the stirred liquid is kept

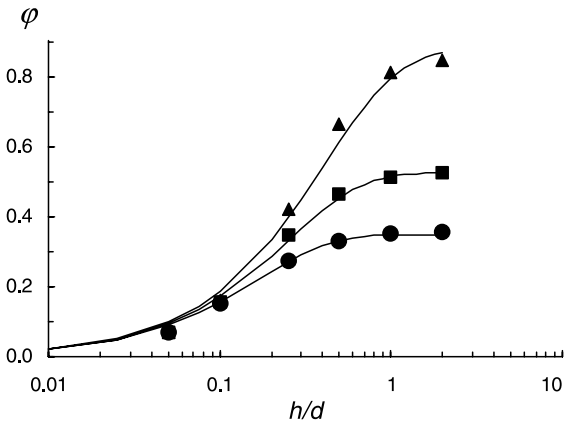

Fig. 6. Correction φ for lateral diffusion for various sample thickness h, width of cathode insulation w and cathode diameter d computed by Fluent (●) $w/d=0.2$; (■) $w/d=0.3$; (▲) $w/d=0.5$; (—) interpolation formula (22).

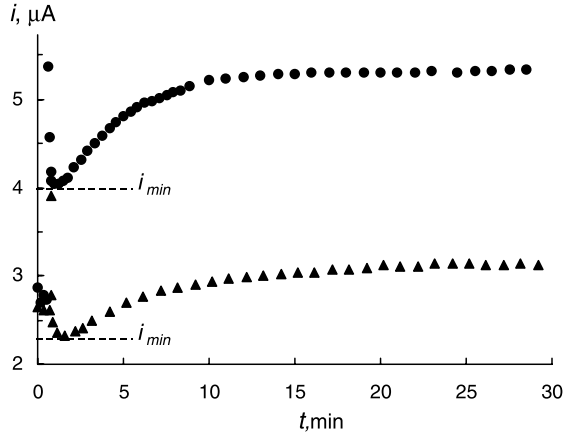

Fig. 7. Typical current response obtained after attachment of the cathode to the polymer. Before the attachment, steady-state oxygen flow with zero oxygen concentration on the polymer surface was maintained by inert gas. PVP (●) $h=1.01$ mm, (▲) $h=1.83$ mm.

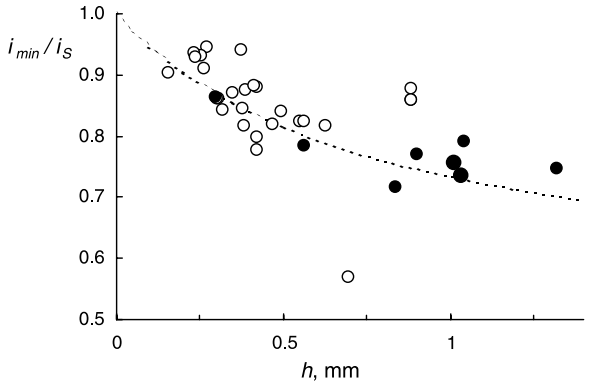

Fig. 8. The check-up of the possibility of fast measurement without edge effects. (●) (○), experimental data, (– – –) $1/(1+\varphi(h))$ by Eq. (22).

under the sample. The large bubble forms at a proper choice of the stirrer speed. Infusion tube leads the presaturated gas (oxygen or air) of constant temperature and flow rate directly into the bubble. The sparse gauze surrounding the bubble space avoids backmixing, which is a potential source of error, until the liquid is fully saturated. In such a way, replacement of gases inside the large bubble is attained almost immediately after the cock switch. Simultaneously, the well-stirred ambient liquid maintains a uniform temperature in diffusion cell and in the polymer sample.

To minimize the effect of external resistance ($R_a = h_a/P_a \to 0$), neither cigarette paper nor a supporting grid was used in most of the runs.

Several experiments were made with silicone rubber discs, $h = 1$ and 4 mm, and with stacked cigarette papers alone.

4. Results and discussion

4.1. Permeability

Eq. (6) can be rearranged for the cathode diameter $d = 2.97$ mm to

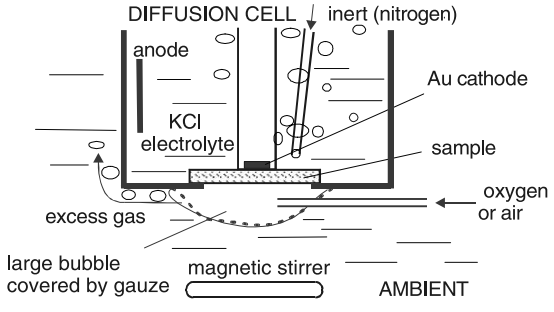

Fig. 9. Arrangement with a gas bubble for the diffusivity measurement.

$$y \equiv \frac{p[\mathrm{hPa}](1+\varphi)}{11178 i_s[\mu\mathrm{A}]} = \frac{1}{P[\mathrm{barrer}]} h[\mathrm{mm}] + R_a \left[\frac{\mathrm{mm}}{\mathrm{barrer}}\right] \quad (24)$$

where φ is given by Eq. (22). Like in most of literature concerning membranes, customary barrer units are used for permeability in Eq. (24).

Note: One barrer corresponds to the oxygen flow 10^{-11} cm^3/s (at standard temperature and pressure) through the area $A = 1$ cm^2 with $h = 1$ cm and $\Delta p = 1$ Torr. To express it in SI units, the conversion factors are:

$$1\ \mathrm{barrer} \equiv 10^{-11}(\mathrm{cm}^2/\mathrm{s})(\mathrm{cm}^3\ \mathrm{O_2}/(\mathrm{cm}^3\ \mathrm{Torr})) = 0.750 \times 10^{-11}(\mathrm{cm}^2/\mathrm{s})(\mathrm{cm}^3\ \mathrm{O_2}/(\mathrm{cm}^3\ \mathrm{hPa})) = 0.335 \times 10^{-15}\ \mathrm{mol}/(\mathrm{ms\ Pa})$$

The two unknown parameters, permeability P and the boundary resistance R_a can be evaluated from measured values i_s and h by linear regression.

Figs. 10 and 11 show the relation between the overall resistance y to oxygen flow and the sample thickness h for eight sets of experimental data obtained for two polymer materials, two electrolyte concentrations and two different resistance configurations (with and without supporting grid and cigarette paper). The data fit well a linear relationship. The obtained values of parameters P and R_a are given in Table 3.

Unexpectedly, oxygen permeability in both hydrophilic polymers depends significantly on the concentration of the electrolyte. This phenomenon can be explained, e.g. by lower swelling of polymer in more concentrated solution or by the effect of salt on oxygen solubility and diffusivity in water itself. The later effect is known for sodium chloride, Table 4. Similar trends can probably be assumed in potassium chloride solution and in hydrogels as well. The effect of electrolyte concentration can be one of the reasons for some scatter in experimental data presented in literature for oxygen permeability in hydrophilic polymers.

The PHEMA with a water content 38% is an accepted standard hydrogel material and its nominal permeability $P = 9.6$ barrer at 35 °C is recommended to be used to check the accuracy of permeability measurements [1,15]. Nevertheless, recent data [16] obtained by the standard method [1] are 10% higher and $P = 10.4$ barrer, is recommended for PHEMA 38%. Our values are close to the later data.

Further, Table 3 shows that all the data obtained for sample arrangement with supporting grid and paper can be described with common parameter $R_a = 0.004 \pm 0.001$ mm/barrer. It has been checked that the boundary resistance pertains mainly to the grid and its adjacent liquid layer, the paper resistance is smaller. Similarly, for all experimental series without the paper and grid, $R_a = \pm$

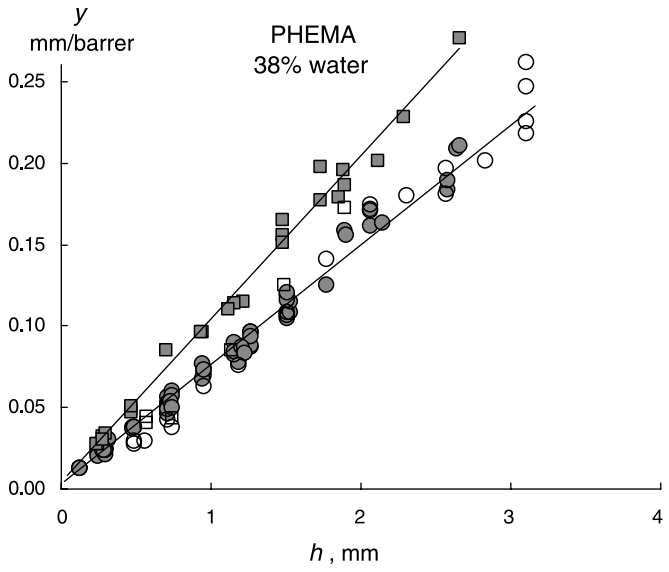

Fig. 10. The overall resistance to oxygen flow as a function of the sample (PHEMA) thickness for various additional resistances and potassium chloride concentrations. (●) 0.1 M KCl, grid and cigarette paper; (○) 0.1 M KCl, paper; (■) 0.5 M KCl, grid and cigarette paper; (□) 0.5 M KCl, paper.

0.001 mm/barrer. Apparently the boundary effects are quite well reproducible in our experimental setup.

Under these conditions, the oxygen permeability in the polymer can be calculated from the steady-state current measured for a single sample of suitable thickness using the equation

$$P = \frac{h}{(zFAp(1+\varphi)/i_s) - R_a} \tag{25}$$

where φ is given by Eq. (22) and R_a is known.

The error in $R_a \pm 0.001$ mm/barrer causes the following uncertainty of permeability determination in our experimental configuration: 10 barrer is obtained for $h=0.2$ mm as 10 ± 0.5 barrer and for $h=2$ mm as 10 ± 0.05 barrer. A less acceptable uncertainty is for samples with permeability 100 barrer, where it makes 100 ± 50 barrer for $h=0.2$ mm and 100 ± 5 barrer for $h=2$ mm. On the other hand, for thick samples with low permeability, error in the value of the background current may also become important.

The advantage of the method with thicker samples is evident for oxygen transport investigation in high-permeable materials.

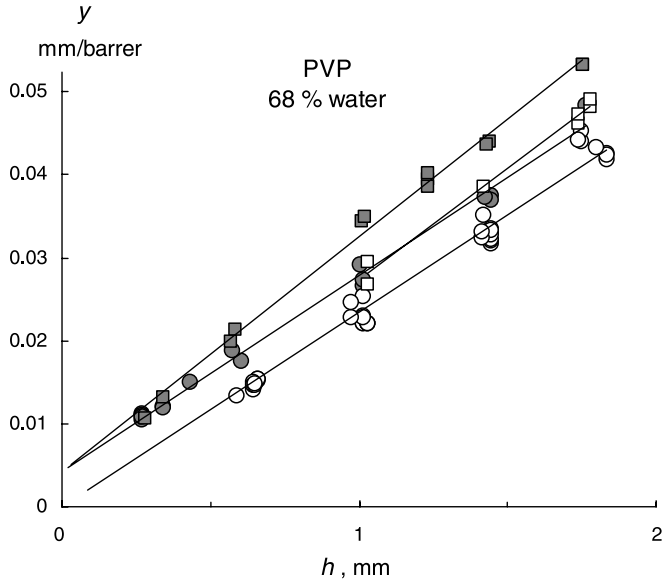

Fig. 11. The overall resistance to oxygen flow as a function of the sample (PVP) thickness for various boundary resistances and potassium chloride concentrations. (●) 0.1 M KCl, grid and cigarette paper; (○) 0.1 M KCl; (■) 0.5 M KCl, grid and cigarette paper; (□) 0.5 M KCl.

Table 3
Oxygen permeability P of hydrogels and boundary resistance R_a with supporting grid and paper

	Electrolyte (mol/dm^3 KCl)	P (barrer)			R_a (mm/barrer)
		Experimental	Prediction [1,15]	Prediction [15]	
PHEMA 38%	0.5	10.5	9.5	10.4	0.0043
	0.1	13.6			0.0030
PVP 68%	0.5	35.3	32.7	35.1	0.0042
	0.1	42.4			0.0043

Table 4
Properties of oxygen in water solutions of NaCl [17–20]

NaCl concentration (mol dm^{-3})	Solubility, k (10^{-6} mol m^{-3} Pa^{-1})		Diffusivity, D (10^{-9} m^2 s^{-1})		Permeability, P (barrer)	
	34 °C	35 °C	34 °C	35 °C	34 °C	35 °C
0	11.14	10.96	3.10	3.21	101.6	103.5
0.1	10.79	10.62	3.06	3.16	97.3	98.9
0.5	9.52	9.38	2.91	3.00	81.7	82.9

4.2. Diffusivity

Three procedures were tested for estimation of the characteristic time t_C from the $\eta(t)$:

(i) Fitting the response with a numerical solution of Eq. (11).
(ii) Integration of $(1-\eta(t))$ according to Eq. (9).
(iii) Calculation from Eq. (13) for known $t_{1/2}$.

No significant shift of the values t_C determined by the (i)–(iii) was beyond the range of experimental error. The typical current response to the step change in oxygen concentration is shown in Fig. 12 for PHEMA sample with thickness 0.837 mm, and for PVP sample with

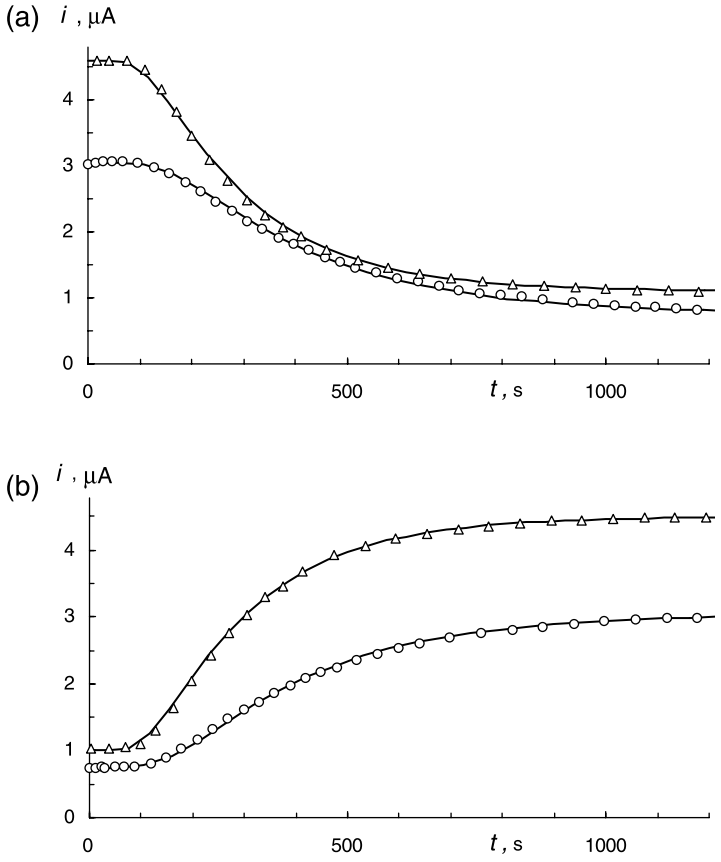

Fig. 12. Current response to the step change in concentration in $t=0$ (a) oxygen–air, (b) air–oxygen (○) PHEMA, $h=0.737$ mm; (Δ) PVP, $h=1.030$ mm; (—) theoretical interpretation by Eq. (11) with $t_C=445$ s for PHEMA and $t_C=320$ s for PVP.

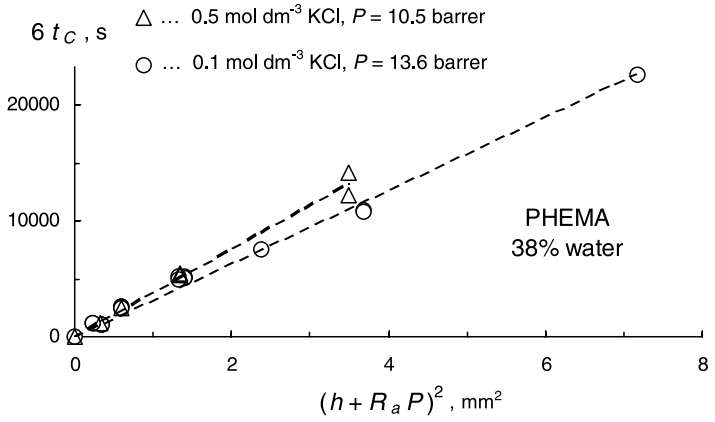

Fig. 13. Dependence of the characteristic time of oxygen transfer through PHEMA sample on sample thickness, $R_a = 0.001$ mm/barrer. (Δ) 0.5 mol dm^{-3} KCl, $P = 10.5$ barrer; (○) 0.1 mol dm^{-3} KCl, $P = 13.6$ barrer.

thickness 1.030 mm. A very good agreement between the measured response and that calculated by the procedure (i), $t_C = 445$ s for PHEMA and $t_C = 320$ s for PVP, also confirms the proposal to describe the $\eta(t)$ by Eq. (11) instead of Eq. (16).

The additional resistance $R_a = 0.001$ mm/barrer or 0.004 mm/barrer for the samples without or with paper and supporting grid, respectively, was taken for evaluation of the oxygen diffusivity D.

The values $6t_C$ obtained for two KCl concentrations are plotted against the $(h+R_aP)^2$ for PHEMA and PVP in Figs. 13 and 14. The data are somewhat scattered, but their trend to fit the expected linear relationship can be seen.

Therefore, the oxygen diffusivity, D, was calculated in accordance with Eq. (19) from the reciprocal value of the line slope

$$D = \left(\frac{\mathrm{d}(6t_C)}{\mathrm{d}\left[(h + R_aP)^2\right]} \right)^{-1} \tag{26}$$

A set of data with cigarette paper and grid, as required for soft materials with low water contents, is also demonstrated in Fig. 14. The slopes of lines with and without additional resistances are the same. This confirms the appropriateness of Eq. (19) also for the conditions, where the influence of R_a is not entirely negligible.

Increasing salt concentration was reflected in decreasing diffusivity and solubility of oxygen in hydrogels similarly as shown in Table. 4 for water and NaCl. A similar tendency is perceptible in Fig. 13 for oxygen diffusivity in PHEMA while with PVP samples measured in a smaller range of thickness the trend is not apparent in Fig. 14.

From the measured dependence of the $6t_C$ on the $(h+R_aP)^2$, the y-intercept

$$y = 3\left(R_aC_a - R_a^2 \frac{P^2}{D} \right) \tag{27}$$

may be obtained by graphical extrapolation of the plot t_C vs. $(h+R_aP)^2$ for $(h+R_aP)^2 \to 0$. Generally, parameter C_a can be calculated from the value of y for known R_a. However, in our experiments, the value y was too small. This did not allow us to determine R_aC_a accurately.

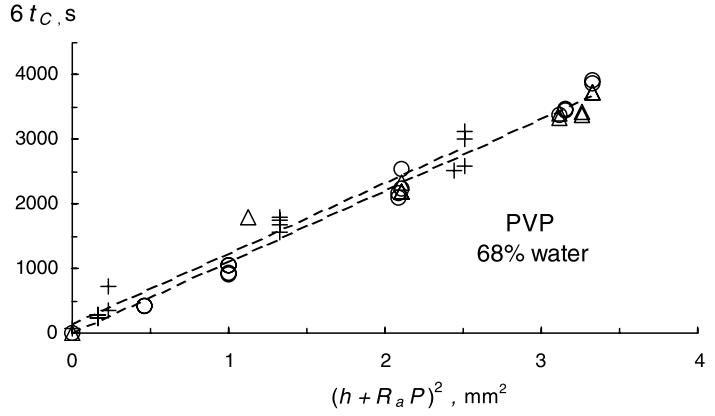

Fig. 14. Dependence of the characteristic time of oxygen transfer through PVP sample on sample thickness. (Δ…) 0.5 mol dm^{-3} KCl, $P = 35.3$ barrer, $R_a = 0.001$ mm/barrer; (○…) 0.1 mol dm^{-3} KCl, $P = 42.4$ barrer, $R_a = 0.001$ mm/barrer; (+…) 0.1 mol dm^{-3} KCl, $P = 42.4$ barrer, $R_a = 0.004$ mm/barrer (sample with paper layer and supporting grid).

Table 5
Permeability, diffusivity and solubility of oxygen in studied materials at 35 °C (0.1 or 0.5 mol/dm^3 KCl in water as an electrolyte)

	P (barrer)	D (10^{-9} m^2/s)	k (10^{-6} mol/(m^3 Pa))
0.1 M NaCl[a]	98.9	3.16	10.5
0.5 M NaCl[a]	82.9	3.00	9.25
PHEMA38/0.1 M KCl	13.6	0.32	14
PHEMA38/0.5 M KCl	10.5	0.27	13
PVP68/0.1 M KCl	42	0.89	16
PVP68/0.5 M KCl	35	0.89	13
Wet paper/0.1 M KCl	34	1.6	7.3
Silicone rubber	500	1.1	150

[a] Ref. [18].

Then solubility of oxygen in the sample is calculated from Eq. (2), $k = P/D$.

All results are presented in Table 5.

5. Conclusion

A polarographic method with inert gas for investigation of oxygen mass transfer in polymers immersed in liquids was developed. Permeability is determined from the current measured under the steady state conditions; diffusivity is determined from the current response at one polymer surface to the step change in concentration at the other one.

In the proposed experimental setup, the liquid around the cathode is saturated with an inert gas. In this way the lateral oxygen diffusion is suppressed and its contribution to the oxygen flow is well defined also for samples thicker than recommended in the standard Fatt method.

Then, the additional resistance of, e.g. cigarette paper, supporting grid and liquid boundary layer is rather constant and it can be determined only once for given experimental conditions. This means that laborious measurements with a series of samples of different thickness need not be performed for each material.

At the beginning of experiment, the inert gas ensures practically zero oxygen concentration at one polymer surface. So, electrochemical measurement itself takes a shorter time period and possible readjustment of the probe on the sample does not require performing the complete time—consuming procedure to attain a steady state again. Also the danger of cathode contamination is lower than in classic longer measurements.

A theoretical solution of unsteady diffusion through polymer and some additional layer has been interpreted to demonstrate quasi-similarity of oxygen flux responses for wide range of conditions. This makes it possible to obtain easily the characteristic time and diffusivity from the half-time of the measured response. The exceptional case where the resistance of additional layer is dominant for the whole range of sample thickness should be avoided; in such a case the diffusivity estimation by the above procedure is too sensitive to any experimental error.

Two standard materials, PHEMA and PVP, were used for testing the suggested method. As electrolyte, potassium chloride solution was used. Essential agreement of oxygen permeability with nominal values in both polymers was obtained for 0.5 M KCl. Oxygen permeability in both polymers for 0.1 M KCl was higher. This difference (20–30%) could be explained by the fact that oxygen diffusivity and solubility in KCl electrolyte decreases with increasing salt concentration, similarly as was found for NaCl solution [17–20]. New data on oxygen diffusivity in standard polymers were obtained.

The method with inert gas has been found suitable for investigation of oxygen transport in biocompatible polymers. It enables simultaneous determination of diffusivity and permeability, which is a unique way to obtain oxygen solubility.

Particular changes in material composition and structure can affect diffusivity and solubility and both these effects should be taken into consideration in design of new biocompatible polymers with desired properties.

Acknowledgements

The authors wish to acknowledge financial support from the Grant Agency of the Czech Republic under project 106/00/1296.

References

[1] Determination of oxygen permeability and transmissibility with the Fatt method, ISO 9913-1/1996.
[2] Permeometer with guard ring cell, Rehder Development Company, http://www.rehder-dev.com/; 2003.
[3] Compañ V, Guzmán J, Riande E. Biomaterials 1998;19:2139–45.
[4] Compañ V, Andrio A, López-Alemany A, Riande E. Polymer 1999; 40:1153–8.
[5] Aiba S, Huang SY. Chem Eng Sci 1969;24:1149–59.
[6] Nicodemo L, Marcone A, Monetta T, Mensitieri G, Bellucci F. J Membr Sci 1992;70:207–15.
[7] Aiba S, Ohashi M, Huang SY. Ind Eng Chem Fundam 1968;7: 497–502.
[8] Nicodemo L, Bellucci F, LeRose R, Carfagna C. J Membr Sci 1989; 43:177–86.
[9] Fatt I. Polarographic oxygen sensors. Cleveland: CRC Press; 1976.

[10] Carslaw HS, Jaeger JC. Conduction of heat in solids. Oxford: Clarendon Press; 1959.
[11] Linek V, Sinkule J, Vacek V. Biotechnol Bioeng 1983;25:1401.
[12] Linek V, Vacek V, Sinkule J, Beneš P. Measurement of oxygen by membrane-covered probes. New York: Prentice Hall; 1988.
[13] Weissman BA, Fatt I, Pham C. J Am Optom Assoc 1992;63: 187–90.
[14] Wichterlová J, Platos P, Otiskova L, Wichtesle K. Proceedings of 50th Conference CHISA, ISBN 80-86059-36-7: V1.31; 2003.
[15] Sarver MD, Baggett D, Harris M, Louie K. J Am Optom Physiol Opt 1981;58(5):386–92.
[16] Young MD, Benjamin WJ. Eye Contact Lens 2003;29(2):126–33.
[17] Perry RH, Green DW. Chemical engineer's handbook. 7th ed. New York: McGraw Hill; 1997.
[18] Ramsing N, Gundersen J. Seawater and gases 2003 [http://www.unisense.com/support/pdf/gas_tables.pdf].
[19] Garcia H, Gordon L. Limnol Oceanogr 1992;37:1307–12.
[20] Li Y-H, Gregory S. Geochim Cosmochim Acta 1974;38:703–14.